Kinetic features of xylan de-polymerization in production of xylose monomer and furfural during acid pretreatment for kenaf, forage sorghums and sunn hemp feedstocks

Srinivas Reddy Kamireddy[1], Evguenii I. Kozliak[2], Melvin Tucker[3], Yun Ji[1*]

(1. *Department of Chemical Engineering, University of North Dakota, Grand Forks, ND 58202, USA*;
2. *Department of Chemistry, University of North Dakota, Grand Forks, ND 58202, USA*;
3. *National Bioenergy Center, National Renewable Energy Laboratory, Golden, CO 80401, USA*)

Abstract: A kinetic study of acid pretreatment was conducted for sorghum non-brown mid rib (SNBMR) (*Sorghum bicolor L Moench*), sorghum-brown mid rib (SBMR), sunn hemp (*Crotalaria juncea L*) and kenaf (*Gossypiumhirsutum L*), focusing on rates of xylose monomer and furfural formation. The kinetics was investigated using two independent variables, reaction temperature (150°C and 160°C) and acid concentration (1 and 2 wt%), with a constant dry biomass loading of 10 wt% and a treatment time up to 20 min while sampling the mixture every 2 min. The experimental data were fitted using a two-step kinetic model based on irreversible pseudo first order kinetics at each step. Varied kinetic orders on the acid concentration, ranging from 0.2 to >3, were observed for both xylose and furfural formation, the values depending on the feedstock. The crystallinity index of raw biomass was shown to be a major factor influencing the rate of both xylose and furfural formation. A positive correlation was observed between the activation energy and biomass crystallinity index for xylose formation.

Keywords: acid pretreatment, sunn hemp, sorghum brown-mid rib (BMR), sorghum non brown- mid rib (SNBMR), kenaf, reaction kinetics, activation energy, reaction order

DOI: 10.3965/j.ijabe.20140704.010

Citation: Kamireddy S R, Kozliak E I, Tucker M, Ji Y. Kinetic features of xylan de-polymerization in production of xylose monomer and furfural during acid pretreatment for kenaf, forage sorghums and sunn hemp feedstocks. Int J Agric & Biol Eng, 2014; 7(4): 86－98.

1 Introduction

The production of fuels and green chemicals from readily available and renewable lignocellulosic biomass is an important step towards domestic energy independence as well as reduction in carbon output[1]. One way of accomplishing this goal is performing a biomass chemical pretreatment followed by enzymatic saccharification and fermentation[2]. Pretreatment is an essential step in biofuel production in order to overcome the recalcitrant nature of biomass. It is commonly performed using either acids, such as dilute sulfuric or phosphoric acid, or alkaline agents, e.g., sodium hydroxide, ammonia or lime[3].

Lignocellulosic biomass is comprised of cellulose, hemicellulose and lignin. Cellulose consists of spacially organized microfibrils, each containing thousands of six-carbon glucose monomers linked with β-glycosidic bonds[4]. Hemicellulose is a heteropolymer of both five and six-carbon monosaccharide molecules[4]. Lignin is a complex hydrophobic polymer of p-hydroxyphenyl, guaiacyl, and syringyl residues; it fills in the spaces between the cellulose fibers and hemicellulose[5].

Received date: 2014-06-17 **Accepted date:** 2014-08-12

Biographies: Srinivas Reddy Kamireddy, PhD, Postdoctoral researcher, research interest: renewable energy. Email: srinivasreddy.kamire@my.und.edu. **Evguenii I. Kozliak**, PhD, Professor, research interest: kinetic modelling. Email: jenya.kozliak@email.und.edu. **Melvin Tucker**, PhD, Senior Scientist, research interest: biomass pretreatment. Email: melvin.tucker@nrel.gov.

*** Corresponding author: Yun Ji**, PhD, Assistant Professor, research interest: renewable energy. Mailing Address: Department of Chemical Engineering, University of North Dakota, 241 Centennial Drive, Grand Forks, ND 58202, USA; Tel.: +1-701-777-4456; Email: yun.ji@engr.und.edu.

The acid pretreatment selectively removes hemicellulose thus leaving lignin and cellulose in the pretreated solid substrate. These pretreated substrates can be further converted into glucose monomers by cleaving glycosidic bonds using cellulases[6]. Then the fermentable sugars, primarily glucose, can be converted into bio-ethanol and other fuels[6]. Dilute acid pretreatment is currently considered the most promising process for commercialization[7]. One of the inherent results of this pretreatment is the hydrolysis of xylan (polysaccharide of xylose) to yield a pentose monosaccharide, xylose. Energy-efficient xylan hydrolysis in pretreatment and subsequent xylose fermentation to xylitol and other value added chemicals enhance the economic feasibility of bioprocess plants.

Kinetic modeling of xylan acid-catalyzed hydrolysis leading to the formation of xylose and its major degradation product, furfural, has been attempted since 1966[8]. It has been performed on a variety of agricultural feedstocks such as aspen, balsam, corn stover, switch grass and miscanthus[9-12]. Previous studies focused on woody biomass such as aspen, balsam, although herbaceous biomass, switch grass, was also considered. The observed process efficiency turned out to be significantly species dependent[12]. For herbaceous biomass, higher acid concentration was found to be essential for high xylose monomer yield, which ranged between 30-80 wt% at low acid concentrations (0.25-0.75 wt%) and required as long as 60-150 min[12]. Based on this information, this study focused on herbaceous species, kenaf, forage sorghum and sunn hemp, using 1-2 wt% acid concentrations.

A recent study showed that a higher efficiency of xylan hydrolysis was essential for achieving higher fermentable sugar yields during the subsequent enzymatic hydrolysis, due to a greater accessibility of cellulose by cellulases[13]. Our previous optimization studies showed that the reaction temperatures of 150-160°C and acid concentration of 1-2 wt% were significant parameters influencing the yield of target products, monomeric carbohydrates. Running the process at temperatures below 140°C yielded high amounts of undesired oligomers[14]. On the other hand, the use of temperatures above 165°C is known to yield significant amounts of carbohydrate degradation products, such as furfural and hydroxyl methyl furfural (HMF) [14]. Thus, within the selected narrow range of temperatures, two approaches could be used to reduce the further xylose degradation, either 1) applying lower acid concentrations (0.25-0.75 wt%) along with longer reaction times (65-120 min) or 2) using higher acid concentrations (1-2 wt%) combined with shorter reaction times (10-20 min). It is the second approach that has been explored in this study. Process kinetics has not been studied for such high severity conditions.

The current study addresses obtaining detailed kinetic parameters using a batch reactor with a solid dry biomass loading of 10 wt%. The simplest kinetic mechanism that is considered in this study is hydrolysis of xylan to xylose with a subsequent de-hydration of xylose to furfural by a two-step pseudo-first order irreversible reaction with Arrhenius-type kinetic constants[10,15]. However, experimental observations suggest that other models that include oligomeric intermediates and parallel reactions of slow and fast reacting hemicellulose phases (biphasic) could describe the reaction[12]. These complex models tends to overpredict the oligomers and under predict the xylose formation[12]. In this study a simple two step kinetic model was considered.

We postulated that the proposed increase of process temperature and acid concentration would simplify the kinetic model, leaving out the oligomers whose formation at high temperature is postulated to be transient, i.e., effectively (kinetically) insignificant. This hypothesis has turned out to be correct[12,13]. The application of a simpler model enabled the separation of the influence of acid concentration and reaction temperature, correlating them with inherent biomass characteristics and finding the best conditions for selective xylose formation, with the minimum yield of furfural. The proposed treatment is specific to the narrow range of high severity conditions but it is this range that shows significant promise for practical biomass pre-treatment. Based on the parameters obtained, practical recommendations on how to meet this goal have been given for each feedstock.

2 Material and methods

2.1 Biomass material

All four crops were grown at the North Dakota State University experimental site in Fargo and Prosper, ND. Biomass feedstocks (plants) were grown in experimental units that were 9.1 m long and 1.5 m wide and consisted of 6 rows spaced 30 cm apart. All entries were harvested in the last week of September; 2-center rows of each plot were harvested manually. The biomass was air dried while being pulverized in a Wiley mill. The particle size distribution ranged between 50 to 100 μm. Samples were stored in zip-lock bags at room temperature for further use.

2.2 Compositional analysis

Composition of the raw kenaf, SBMR, SNBMR and sunn hemp was assessed according to the National Renewable Energy Laboratory (NREL) Laboratory Analytical Procedure (LAP) protocol (NREL/TP-510-42619). A two-stage extraction process (12 h of water extraction followed by 8 h of ethanol extraction) was performed to remove extractives using a Soxhlet apparatus (Sigma Aldrich, St. Louis, MO). The weight of each biomass sample considered for the analysis was 6.0 g. The feedstock carbohydrate composition is summarized in Table 1.

Table 1 Feedstock composition analysis

	Dry wt%							
Species	Glucan	Xylan	Galactan	Mannan	Arabinan	Lignin	Ash	Extractives
SNBMR	33.9±0.5	15.2±0.2	4.2±0.1	3.8±0.1	0.5±0.1	15.8±0.4	3.3±0.3	26.0±0.1
SBMR	33.7±0.8	13.0±0.6	4.5±0.1	3.8±0.2	0.6±0.1	13.9±0.4	4.2±0.1	25.4±0.6
Sunn hemp	37.1±0.8	9.9±0.5	6.1±0.1	5.4±0.1	0.3±0.1	13.8±1.1	5.2±0.3	22.6±0.2
Kenaf	42.5±4.2	13.5±1.2	2.2±0.4	0.4±0.1	0.7±0.3	17.2±2.1	0.3±0.1	21.0±1.0

Only the main carbohydrate composition was quantified as the focus was made only on the xylan hydrolysis. The glucan and lignin contents were found to be larger in kenaf than in the other feedstocks considered. The amount of structural ash ranged from 0.3 to 5.5 wt%. Such a low ash content allows for performing reproducible acid pretreatment whereas the high ash content, above 10 wt%, might neutralize some of the acid added[16].

2.3 Pretreatment experiments

The biomass pretreatment was conducted in a jacketed batch reactor with a 300-mL internal volume manufactured by Auto Clave Engineers, Erie, PA. The reactor was made of Hastelloy C-276 to mitigate the acidic corrosion at high temperatures. The biomass loading of 10 wt% on dry basis was added to an appropriate amount of 1.0% or 2.0 wt% sulfuric acid, which was prepared by mixing deionized water and sulfuric acid purchased from Sigma Aldrich (St.Louis, MO). The heating source used for the reactor was saturated steam drawn into the reactor's jacket by a three-way valve. More detailed information regarding the reactor schematic and setup was published elsewhere[7]. The agitation rate in the reactor was maintained constant at 60 rpm throughout the reaction. The reactor heating rate was (35±3) °C/min. Once the desired temperature was reached, it was maintained constant and the reaction time commenced. At the allotted times, the reactor was cooled by passing tap water into the external jacket. Once the reactor was cooled below 40°C, the reaction slurry was discharged and collected in a polyethylene bottle for further analysis. The temperature data were recorded with the aid of Picolog software throughout the reaction time. All experiments were duplicated.

The varied operational conditions are listed in Table 2. Each pretreatment experiment was performed up to a maximum reaction time of 20 min. The liquid hydrolyzate samples of each biomass were withdrawn every 2 minutes. There was no detectable pressure or temperature drop during sampling. Select experiments essential for model verification were performed at 155°C, with 1.5 wt% acid concentration for 10 min. The temperature range used could not be expanded as it would alter the process mechanism, see Results and Discussion.

Table 2 Pretreatment conditions employed for each biomass

1 wt% Acid Concentration	2 wt% Acid Concentration
150°C	150°C
160°C	160°C

2.4 Analytical procedures

Pretreated slurry samples were vacuum-filtered and collected as liquid hydrolyzates and solid substrates. The liquid hydrolyzate samples were analyzed for xylose and furfural based on the NREL analytical procedures (NREL/TP- 510-42623). The quantitative analysis of monosaccharides present in liquid hydrolyzates was performed by an Agilent 1200 HPLC with a Transgenomic CHO-Pb 300×7.8 mm column (Omaha, NE). All HPLC analyses were replicated; the resulting variance due to analysis was significantly smaller than the sample-to-sample variation. The mobile phase was deionized water with a flow rate of 0.6 mL/min[17]. Prior to analyzing pretreated hydrolyzate samples, a set of standards were run to calibrate the HPLC Refractive Index Detector. The standard concentrations ranged from 0.5 to 18 g/L. In addition, an internal sugar calibration standard with a concentration of 4.0 g/L was run on every 8th injection to test for column and RID validity. The standard solutions and sugar calibration standard consisted of D-(+) glucose, D-(+) xylose, D-(+) galactose, L-(+) arabinose, and D-(+) mannose.

Furfural was analyzed using an Agilent 1200 HPLC with a 100 × 7.8 mm Phenomenex Rezex RFQ column (Torrance, CA). The 0.01N sulfuric acid mobile phase with a flow rate of 1.0 mL/min was used for analysis [17]. The calibration standards for furfural were obtained from Absolute Standards, Inc (Hamden, CT). The standard concentration for furfural ranged from 0.2 to 6 g/L. The amount of leftover xylan that was retained in the solid substrate after the pretreatment was measured by subtracting the xylose measured in the liquid medium from the xylan found in the original biomass.

2.5 Kinetic model and statistical data analysis

A pseudo first order irreversible reaction model proposed earlier[10,18] was used, which follows the Arrhenius-type kinetics with the mechanism including the hydrolysis of xylan in hemicellulose into xylose monomer and its subsequent degradation into furfural, see Equation (1)[10].

$$X \xrightarrow{k_1} X_m \xrightarrow{k_2} F \tag{1}$$

where, X stands for initial xylan; X_m is the xylose monomer and F stands for furfural.

The kinetic coefficients, k_i, are pseudo-first order constants of the corresponding reactions,

Rate of xylose formation = k_1 $[X]$

Rate of xylose degradation = k_2 $[X_m]$

where the brackets designate the concentration, mol/L, of the corresponding chemical.

The xylan concentration $[X]$ was calculated in the prior work at the conditions studied for kinetic model[19,20]. $[X_m]$ and $[F]$ concentrations can be described by the following equations.

$$\frac{d[X]}{dt} = -k_1[X] \text{ with } [X](0) = [X_o] \tag{2}$$

where $[X]_o$ is the initial xylan concentration;

$$\frac{d[X_m]}{dt} = k_1[X] - k_2[X_m] \text{ with } [X_m](0) = 0 \tag{3}$$

$$\frac{d[F]}{dt} = -k_2[X_m] \text{ with } [F](0) = 0 \tag{4}$$

By solving linear differential Equation (2)-(4) with their corresponding initial conditions, the time dependent expressions below are readily obtained.

$$[X](t) = [X_o] \times e^{(-k_1 t)} \tag{5}$$

$$[X_m](t) = \frac{k_1}{k_2 - k_1} \times (e^{(-k_1 t)} - e^{(-k_2 t)}) \times [X_o] \tag{6}$$

Since

$$[F] = [X_o] - [X_m] - [X] \tag{7}$$

$$[F](t) = \left(1 + \frac{k_1 \times e^{(-k_2 t)} - k_2 \times e^{(-k_1 t)}}{k_2 - k_1}\right) \times [X_o] \tag{8}$$

Equation (8) is obtained as an analytical solution of Equation (5) and (6).

During pretreatment, acetic acid could be produced as a result of hydrolysis of acetyl linkages that are bound to hemicellulose[21]. This acid could act as an inhibitor during the subsequent fermentation process of the pretreated liquid hydrolyzates, as it tends to affect the cell metabolism by lowering the pH[22]. Studies indicate that the processes in which the generation of acetic acid is significant do not follow Equation (1)[23]. However, fewer acetyl groups are known to be present in the backbone of agricultural residues such as SBMR, SNBMR, kenaf and switch grass considered in this study as compared to hardwoods such as aspen and balsam[22]. Hence, the formation of acetic acid is not included in the proposed model. The amount of xylose was calculated

as a mole equivalent of xylan, by applying the ratio of the xylan unit and xylose molecular weights (0.88) as shown in Equation (9) where $[X_m]$ is the concentration of xylose monomer.

$$\text{xylose yield \%} = \frac{[X_m]\times \text{volume of solution for pretreatment}\times 0.88}{\text{weight of starting xylan}}\times 100 \quad (9)$$

The furfural yield was calculated as a mole equivalent of xylose, by applying the ratio of its molecular weights of furfural and xylose to express it as xylose equivalent (1.56) as shown in Equation (10) where $[F]$ is the furfural concentration in the liquid hydrolyzate after the biomass pretreatment.

$$\text{furfural yield \%} = \frac{[F]\times \text{volume of solution used for pretreatment}\times 1.56}{\text{weight of starting xylose}}\times 100 \quad (10)$$

A fraction of the furfural present in hydrolyzates may have originated from the degradation of the other aldopentose occurring in hemicellulose, arabinose[10]. However, arabinan, the essential arabinose precursor, was present only in trace amounts (≤ 1 wt%) in all feedstocks as evident from Table 1. Hence, the contribution of arabinose degradation was ignored. The data sets for each of the four severity conditions studied for each species were fitted using the Lavenberg-Marquardt non-linear curve fitting method in *Mathcad15* (Needham, MA). The kinetic coefficients obtained are functions of temperature, acid concentration and inherent factors according to the Arrhenius equation, Equation (11)[10].

$$k_i = A\, e^{(-\frac{Ea}{RT})} \quad (11)$$

$$A = A_o[C]^{n_i} \quad (12)$$

where, T is the absolute temperature (K); C is the acid concentration in wt %; A is the effective pre-exponential factor (per min); n_i is the reaction rate order (dimensionless); E_a is the Arrhenius activation energy (kJ/mol); R = 8.3143 × 10^{-3} (universal gas constant, kJ/mol-K) and A_o is the inherent (concentration-independent) pre-exponential factor. Model parameters A_o, n_i, and E_i for both xylose formation and xylose degradation were fitted for each species. Since the acid concentration is traditionally measured in wt% as opposed to molar concentrations, the numerical values and units of A and A_o differ from those used in chemical kinetics. However, the values of two most important parameters, n_i and E_a, maintain their physical significance. This feature will be used henceforth to provide valuable mechanistic information and practical recommendations.

F-test based on the calculation of matching the squared variance for the theoretical model and experimental data was used to validate the model because the alternative linear regression might skew the data points[24]. Experimental variance was calculated as one standard deviation of the mean.

3 Results and discussion

3.1 Determination of reaction kinetic parameters

The rate coefficients obtained according to Equation (1) for all feedstocks are listed in Table 3. These rate constant values follow a similar pattern to that reported in the earlier studies conducted on aspen, corn stover, balsam and switch grass; namely, k_1 is greater than k_2 for any given feedstock, both constants increasing with the increase of either acid concentration or reaction temperature[25].

Table 3 Kinetic coefficients obtained using the model described by Equations 5-8

Acid conc† wt%	k_i, s^{-1}	SNBMR		SBMR		Sunn hemp		Kenaf	
		150°C	160°C	150°C	160°C	150°C	160°C	150°C	160°C
1	k_1	1.32×10^{-1}	1.37×10^{-1}	8.39×10^{-2}	1.01×10^{-1}	1.11×10^{-2}	2.50×10^{-2}	6.35×10^{-2}	9.32×10^{-2}
	k_2	1.55×10^{-2}	1.75×10^{-2}	3.30×10^{-3}	8.90×10^{-3}	1.00×10^{-3}	5.00×10^{-3}	2.90×10^{-3}	3.10×10^{-3}
Ratio	k_1/k_2	8.52	7.83	25.4	11.4	11.1	5.00	21.9	30.1
2	k_1	1.51×10^{-1}	1.67×10^{-1}	1.35×10^{-1}	1.58×10^{-1}	1.01×10^{-1}	1.04×10^{-1}	1.19×10^{-1}	1.41×10^{-1}
	k_2	2.74×10^{-2}	3.09×10^{-2}	3.03×10^{-2}	4.60×10^{-2}	7.80×10^{-3}	1.05×10^{-2}	1.80×10^{-2}	3.05×10^{-2}
Ratio	k_1/k_2	5.51	5.40	4.46	3.43	12.95	9.90	6.61	4.46

Note: †=concentration.

The obtained numerical values of rate coefficients were also similar to those reported in the earlier studies on various other biomasses[12,18]. The observed differences between the rate coefficients for various feedstocks suggest a significant variation in the component distribution and lignocellulosic structure arrangement as suggested earlier[12].

The maximum xylose yields for kenaf, SNBMR, SBMR and sunn hemp are tabulated in Table 4. The observed product yields correlated with the obtained corresponding kinetic coefficients, i.e., specific reaction rates, k_1 Table 3. Since the first-order kinetic constant, at a given time, reflects the natural logarithm of the ratio of the initial and final reactant concentrations as expressed in Equation (5), i.e., the product yield, the observed correlation of these two parameters was expected. The significance of this correlation is that it shows that the process occurs under kinetic, as opposed to thermodynamic, control, thus justifying the use of irreversible kinetics in the proposed model.

Table 4 Maximum yields of xylose and furfural for four feedstocks obtained under the listed reaction parameters

Biomass	Acid Concentration in wt%	Reaction Temperature /°C	Reaction time /min	Maximum xylose yield /wt%
SNBMR	1	150	18	76.9±0.5
SBMR	1	150	20	77.9±1.9
Sunn Hemp	2	160	20	72.1±0.3
Kenaf	1	160	20	80.2±1.1

The only exception from this trend was kenaf, for which the highest xylose yield was obtained yet the values of k_1 were smaller than those of SNBMR and SBMR. However, this exception can be explained by a rather slow furfural formation at the lowest acid concentration considered, as further developed in the sections on the acid concentration and temperature. Note that the maximum xylose yield upon kenaf hydrolysis was obtained at a higher temperature than that of SNBMR and SBMR; the xylose yields obtained correlated with the corresponding values of k_1. However, sunn hemp required a higher acid concentration compared to other biomasses. This observation may indicate that there is diffusion limitation for hydronium ions to cleave hemicellulose due to a higher crystallinity index of sunn hemp. Hence, 1 wt% acid concentration was not sufficient to hydrolyze xylan. This is the reason for sunn hemp having a lower rate of xylan hydrolysis as compared to other feedstocks as observed from Table 3. The maximum furfural yields obtained experimentally were 46.2±0.3, 36.5±0.1, 33.4±0.4, 10.1±0.2 % for SNBMR, SBMR, kenaf and sunn hemp. The conditions for obtaining these yields were 160°C and 2 wt% acid concentrations for all feedstocks, i.e., the maximum severity treatment conditions.

3.2 Model justification

Figures 1 and 2 depict the experimental data for xylose formation and degradation, respectively, as well as their match with the kinetic curves obtained upon using the model parameters. In case of SBMR, the model tends to slightly underpredict the xylose and overpredict the furfural formation at the highest acid concentration for intermediate times. Apart from this slight discrepancy, the model was in good agreement with the experimental data for both xylan hydrolysis into xylose monomer and its subsequent de-hydration to furfural.

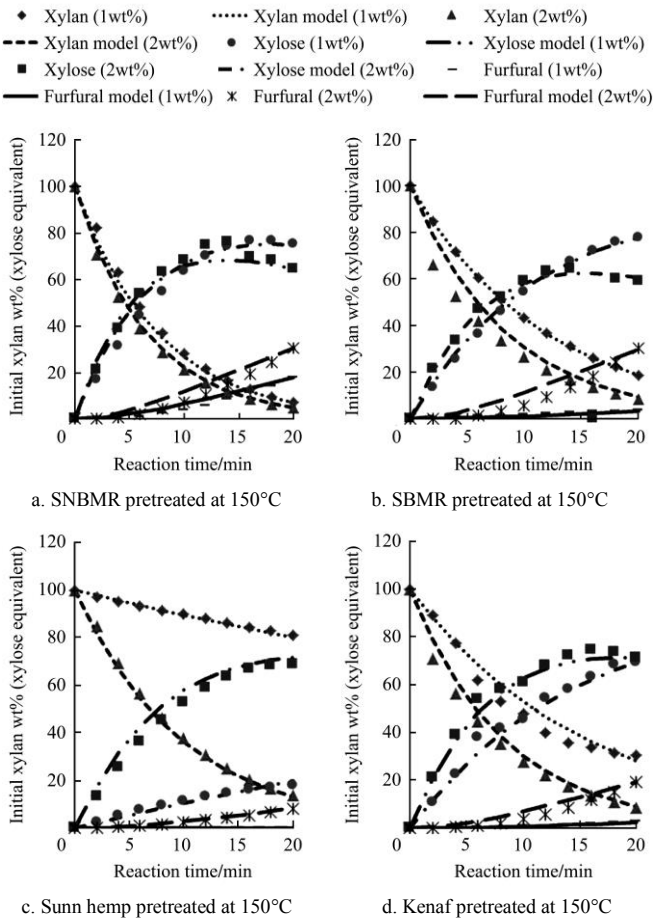

Figure 1 Model prediction and experimental data for xylan, xylose and furfural concentration profiles at 150°C at 1wt% and 2wt% acid concentration

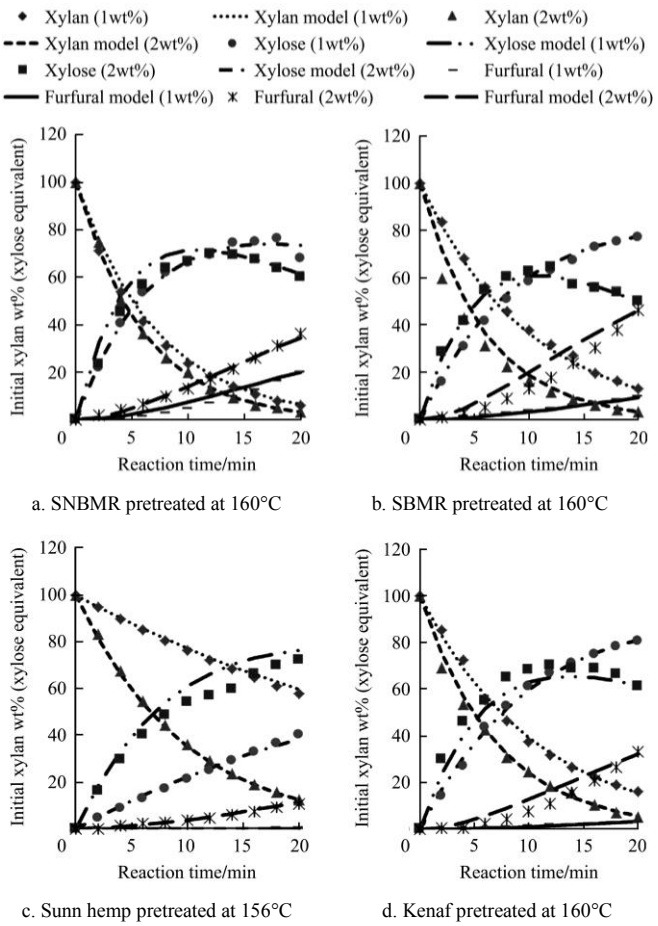

Figure 2 Model prediction and experimental data for xylan, xylose and furfural concentration profiles at 160°C at 1wt% and 2wt% acid concentrations

As can be seen in Figures 1 and 2, a satisfactory stoichiometric balance on of xylan in the solid fraction was obtained, thus justifying the use of the simplified, two-step model (downplaying the oligomer formation), just as was postulated for the selected high-temperature treatment. The complete mass balance closures for all the feedstocks were conducted in prior studies with 95.3±4.1 wt% for the conditions used in this study[19,20].

The next question in model validation was whether the obtained kinetic parameters listed in Table 5 could be varied without significantly altering the match with experimental data. Two approaches were used to address this issue. First, the F-test was conducted, i.e., minimizing the sum of squared errors (SSE) between the theoretical model and the experimental data by varying the pre-exponential factor, activation energy and reaction order on the acid concentration[22,24]. Table 6 lists the SSE corresponding to the best-fit values described by Eq. (11). The difference in variance between the experimental rate coefficient and model was low as evident from Table 6. The data sets either passed the F-test ($F<F_{critical}$) or nearly passed it[22]. One of the instances when $F>F_{critical}$ was the xylose formation from SBMR mentioned in the previous paragraph. The other two cases were the furfural formation from sunn hemp and xylose formation from kenaf; however, the corresponding panels of Figures 1 and 2 show that these deviations resulted from a small bias observed only at intermediate time values. It is of note that an alternative model based on parallel rather than sequential reactions led to an order of magnitude higher variance, with a poor fit of experimental data[18]. Thus, the applied model can be deemed adequate, given the inherent homogeneity of the system used.

Table 5 Fitted Arrhenius parameters obtained from Equations (11) and (12) from the kinetic coefficients listed in Table 3

	Xylose formation			Xylose degradation		
Biomass	n_1	A_{01} (1/min)	E_1 (kJ/mol)	n_2	A_{02} (1/min)	E_2 (kJ/mol)
SNBMR	0.2	11.5	15.7	0.5	4.45×10^4	52.3
SBMR	0.6	76.4	24.0	3.2	2.35×10^5	63.6
Sunn hemp	2.8	622	38.0	1.6	5.08×10^7	84.3
Kenaf	0.9	108	26.2	2.6	2.41×10^7	80.4

Table 6 Sum of squared errors and *F* values for the experimental and model parameters

Biomass		SSE	Variance for Experimental parameters	Variance for model	*F* value	*F* critical
SNBMR	k_1	4.4×10^{-4}	2.4×10^{-4}	1.8×10^{-4}	1.36	9.27
	k_2	4.5×10^{-5}	5.6×10^{-5}	2.7×10^{-5}	2.01	9.27
SBMR	k_1	1.0×10^{-5}	1.1×10^{-3}	1.1×10^{-3}	0.96	0.10
	k_2	4.9×10^{-5}	3.8×10^{-4}	3.4×10^{-4}	1.12	9.27
Sunn Hemp	k_1	4.9×10^{-5}	2.4×10^{-3}	2.1×10^{-3}	1.12	9.27
	k_2	1.5×10^{-5}	1.6×10^{-5}	2.4×10^{-5}	0.66	0.10
Kenaf	k_1	2.9×10^{-4}	1.1×10^{-3}	1.5×10^{-3}	0.76	0.10
	k_2	4.0×10^{-6}	1.7×10^{-4}	1.7×10^{-4}	1.03	9.27

Second, the observed reaction orders were verified by replacing the obtained numerical values of n_i with the kinetically relevant integers (0, 1, 2) in Equations (11) and (12) and running the model with these artificially set values. This led to poor predictions of the rate coefficients, leading to a significant failure of the F-test; furthermore, in most of the cases the activation energies obtained with such set values of parameter *n* turned out to

be *negative*. This, in turn, would suggest that the reaction rate decreases with an increase in temperature, which is just the opposite to what was observed Table 3.

To further validate the obtained kinetic model parameters, an independent series of experiments was performed at a different temperature, 155°C, for 10 min at 1.5 wt% acid concentration. The yields of both xylose and furfural were determined experimentally and then compared with those predicted by the model for this particular set of parameters, of Table 5. The results of this comparison shown in Table 7 demonstrated that the model predictions were reasonably accurate for the xylose yield. The furfural yields were slightly overestimated, although the qualitative trends were still predicted. This slight overestimation indicates that the rate of furfural formation increases with temperature even steeper than the exponential Arrhenius function; the values measured for 160°C were higher than those for 155°C. This observation defines the limits of not only the use of the suggested model but also of the process. Selective xylan hydrolysis to xylose should not be conducted at temperatures significantly exceeding 160°C.

Table 7 Validation of the kinetic parameters with the samples pretreated at 155°C for 10 min at 1.5 wt% acid concentration

Biomass	Xylose (predicted)	Xylose (experimental)	Furfural (predicted)	Furfural (experimental)
SNBMR	64.5	68.7±3.2	6.2	2.1±0.2
SBMR	59.7	65.8±2.8	4.18	1.5±0.4
Sunn hemp	57.5	51.4±3.4	1.28	0
Kenaf	63.6	58.6±1.7	5.2	1.3±0.1

Hence, it could be concluded that the kinetic parameters, including the effective rate orders predicted by the model and listed in Table 5 are significant and accurate. Note that standard deviations for these computer-generated model parameters cannot be provided as they are not obtained experimentally. The following sections analyze, one by one, the main factors affecting the reaction rates, i.e., the rate order on the acid concentration and activation energies, as well as their correlation to the biomass parameters.

3.3 Influence of reaction order on the acid

The most characteristic and unusual kinetic feature observed was the occurrence of high kinetic orders on the acid concentration suggesting a simultaneous action of several proton donors on the functional groups near the bond to be broken at the rate-limiting step. Due to the inherent sample heterogeneity, the observed numerical values (Table 5) reflect effective mean values, so they are not necessarily integers. The observed significant variation of this kinetic parameter indicates that the reaction mechanisms of various crops pre-treatment differ in details. For instance, the n_i values for SNBMR were found to be lower than 1 for both xylose formation and xylose degradation; they deviated considerably from the rest of crops. This difference suggests that hemicellulose in SNBMR does not require a concerted attack of several acid molecules, i.e., occurs readily. As shown previously in the literature, native xylan is not homogeneous and could be represented as a combination of fast and slow reacting polysaccharide[23]. Thus it appears that the fast reacting xylan is more abundant in SNBMR as compared to the other crops considered.

The values of n_i for the rest of the crops were found to be larger than those observed in the earlier studies conducted on aspen, balsam, bass wood, red maple, switch grass, even though most of these feedstocks consisted of woody biomass, which is expected to be more resistant to pre-treatment[12,18]. The apparent reason is that those studies used lower acid concentrations (<0.8wt%). Perhaps, a new mechanistic path is enabled at higher acid concentrations (apparently above a certain threshold acid concentration value), allowing for a more efficient treatment of the slow-reacting xylan fraction[25,26].

To confirm this hypothesis, the same kinetic parameters as those used in this study are listed in Table 8 for the earlier studies conducted at lower acid concentrations (<0.8wt%). It can be seen from Table 8 that the lower xylan hydrolysis rates observed under such conditions result from not only lower kinetic orders on acids but also from significantly higher Arrhenius activation energies than those observed in the current study, of Table 5. Thus, increasing the acid concentration appears to enable the otherwise inaccessible path with a lower activation energy barrier, just as suggested.

Table 8 Kinetic parameters reported in literature obtained at lower acid concentrations (< 0.8 wt%) for activation energy and reaction order [12]

Biomass	CrI‡	Ea for Xylose Yield (kJ/mol)	Reaction Order for Xylose Yield	Ea for Furfural Yield (kJ/mol)	Reaction Order for Furfural Yield	References for crystallinity index
Aspen	47%	69	1.22	132	1.2	27
Balsam	49%	84	1.33	125	1.55	28
Switch Grass	69%	89	2.47	106	0.06	29

Note: ‡=Crystallinity Index.

The observed difference in reaction orders on the acid concentration between xylose and furfural formation (Table 5) presents an opportunity for achieving higher yields of the intermediate, xylose, at the expense of furfural. Such "optimum" xylose yields, i.e., those with a reasonable xylan conversion yet with less than 5% furfural yield, are listed in Table 9 along with the reaction conditions leading to such yields. The resulting low furfural concentrations, less than 3-4 g/L, would not lead to any adverse effects on *Saccharomyces cerevisiae* strains, as they were shown to perform efficient fermentation into bio-ethanol under such conditions for liquid hydrolyzate samples[30].

Table 9 Optimum xylose yield conditions based on <5 wt% furfural yield for four feedstocks

Biomass	Acid concentration in wt%	Reaction Temperature/°C	Reaction time/min	Maximum xylose yield/wt%
SNBMR	1	150	10	63.4±0.2
SBMR	1	150	20	77.9±1.9
Sunn Hemp	2	150	14	63.6±0.7
Kenaf	1	150	10	69.3±0.4

As evident from Table 5, SBMR and kenaf featured higher values of n_2 for furfural formation compared to n_1. Conversely, sunn hemp requires a higher acid concentration to be converted to xylose as evident from the values of n_1 shown in Table 5; a significant accumulation of xylose would occur even at a higher acid concentration. This suggestion corroborates the conditions under which the maximum xylose yield was achieved for sunn hemp (Table 4). By contrast, for SNBMR the observed similarity of n_1 and n_2 values (Table 5) significantly hinders the separation of two sequential steps, which leads to lower xylose yields under any conditions; this feature explains the low optimum xylose yield for this feedstock (Table 9).

However, according to Table 9, temperature is even more important. To reduce the furfural formation, a low reaction temperature, particularly in combination with longer reaction times, should be considered for the pretreatment of the above mentioned feedstocks. This recommendation is enhanced by the consideration of activation energy values, which is provided in the next section. As shown in the next section, the model applied allows for the decomposition of the commonly used single lumped severity factor into its components.

3.4 Effect of temperature

For any given feedstock, the values of Arrhenius activation energy were lower for xylose formation than for its subsequent hydrolysis (Table 5), indicating that furfural should be formed at greater amounts at higher temperature as the ratio of k_1/k_2 always decreased with increase in temperature as evident from Table 3. This conclusion corroborates the trends in product yields observed in the current study (Table 4) as well as the published information[18]. The E_a values for xylose formation were found to be significantly lower than those of xylose degradation, with the difference exceeding 35 kcal/mol. Given such a large ΔE_a value between the reactions of xylose formation and decomposition, even a small increase in temperature would be expected to significantly increase the yield of furfural. The ΔE_a value is particularly large for kenaf (54 kcal/mol), explaining the observed largest yield of xylose before it converted to furfural (Table 4). Perhaps, crops with the maximum ΔE_a value may be most applicable for this scenario. For the feedstocks with low ΔE_a values, the application of low reaction temperatures under longer reaction times is particularly advised.

However, if only the temperatures were varied and the acid concentrations were a less significant factor, the yields of xylose and furfural would exhibit similar trends for all feedstocks. The observation that, countering this assumption, the maximum yield of xylose was still

obtained at a higher temperature for sunn hemp, further emphasizes the importance of acid concentration as a separate parameter, as shown in the previous section. This observation also led us to the consideration of dependence of reaction kinetic parameters on the inherent biomass parameters.

3.5 Effect of biomass crystallinity

The kinetic parameters obtained in this work should not be viewed as fundamental constants. Due to the inherent features of biomass as a complex chemical matrix, they are merely effective parameters valid only for a particular crop within the given range of temperature and acid concentrations. Given this limitation, attempts to correlate the obtained kinetic constants with any features of feedstock composition listed in Table 1 were unsuccessful. However, the values of both k_1 and k_2 consistently increased with a decrease of the raw biomass crystallinity index, which is 81.26%, 48.20%, 37.02% and 32.58% for sunn hemp, kenaf, SBMR and SNBMR, respectively[31-33].

In an attempt to separate the influence of acid concentration and temperature on the rate of xylose and furfural formation, both n_i and E_a were plotted vs. the biomass crystallinity in Figures. 3a and 3b, respectively. Figure 3a shows that the activation energies of both reactions increase along with the biomass crystallinity index. This result was expected for the first reaction since most of the hemicellulose that contains xylan is bonded to crystalline cellulose through hydrogen bonds. It is less intuitive for the furfural formation because one might assume that once xylose is released into the solution, the crystallinity index should not play a major role. The obtained results indicate that the xylose formed remains encased in water-insoluble cellulose, which appears to hinder the access of hydronium ions to this essential precursor of furfural. The alternative explanation assuming the parallel rather than sequential furfural formation directly from xylene failed to describe the experimental data as mentioned earlier.

As for the reaction order on the acid, a positive correlation with the biomass crystallinity index was observed for xylan to xylose hydrolysis, n_1 (Figure 3b). The initial hydrolysis of xylan to xylose is indeed expected to be hindered by a higher biomass crystallinity as the simultaneous action of multiple hydronium ions becomes essential to hydrolyze a more stable xylan fraction embedded into crystalline clusters. By contrast, the rate order for xylose to furfural conversion, n_2, showed no correlation with the crystallinity index. Thus, the remaining cellulose appears to be detached from the xylose formed, acting more like a mechanical rather than chemical barrier in more crystalline structures; so just higher temperature but no extra hydronium ions are required to produce furfural.

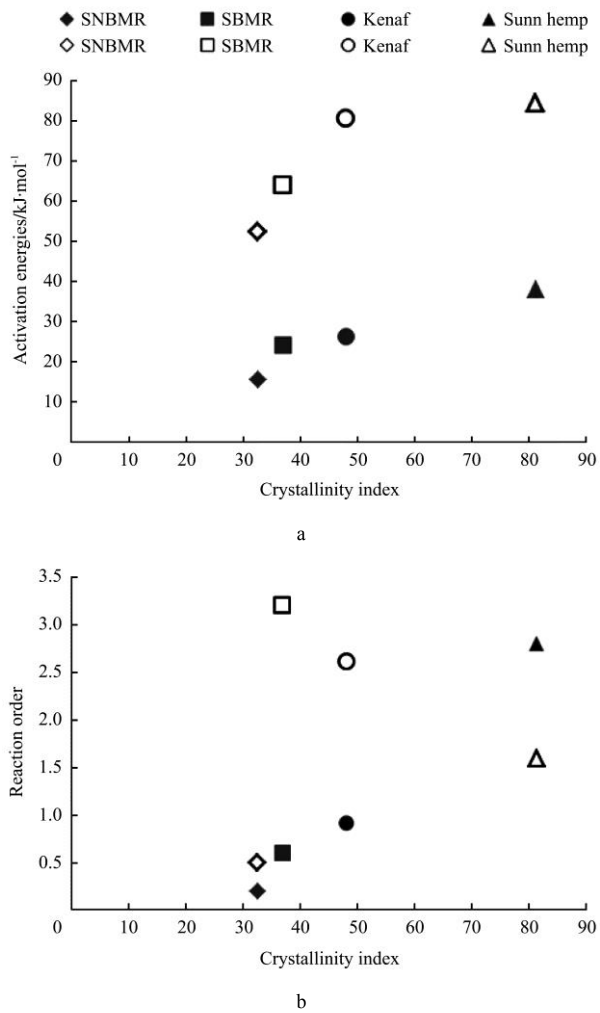

Figure 3 The effect of crystallinity index on a) activation energy for both E_1 (closed symbols) and E_2 (open symbols); b) reaction order on the acid concentration, n_1 (closed) and n_2 (open) for four feedstocks

The kinetic parameters obtained in other works at lower acid concentrations (Table 7) show direct correlations with the crystallinity index only for E_{a1} and n_1, i.e., xylan hydrolysis, but not for furfural formation. This difference may be interpreted as that the low-acid

treatment leaves a fraction of xylose being trapped within the cellulose sheath, thus rendering it inaccessible to further conversion, unlike the high acid concentration process[12].

Apart from the crystallinity index, other factors can influence the xylan hydrolysis, such as 1) diffusional limitations of hydronium ions' mobility; 2) non-homogenous reactions at the xylan- water interface[34] or even the distribution of crystalline zones rather than their absolute abundance. However, both of these factors may be linked to biomass crystallinity. For example, the activation energies for the first reaction, i.e., xylan hydrolysis, are so low in the least crystalline biomasses, SBMR and, in part, SNBMR and kenaf, that this process may be diffusion-limited thus explaining the observed low values of n_1 for these feedstocks, as opposed to more crystalline sunn hemp (Figure 3a).

3.6 Practical implications for pretreatment

Unlike the earlier proposed detailed models accounting for the formation of xylose oligomers, the simplified model used allows for making practical recommendations because the indexes "1" and "2" in all kinetic parameters are directly related to the first and second reactions of Equation (1) within the considered narrow range of high severity conditions. The oligomer formation as well as the availability of several paths of xylan hydrolysis are still reflected in the effective values of kinetic parameters, n_i and E_a. The model also separates the influence of temperature and acid concentration on the rates of these two reactions.

The following recommendations directly based on the model can be made for optimizing the xylose formation: a) lower acid concentrations and lower reaction temperatures are required for SNBMR hydrolysis; b) for SBMR and kenaf, higher acid concentration and low temperature are recommended; c) sunn hemp treatment would benefit from higher reaction temperatures and higher acid concentrations. If, conversely, the bio-refinery goal is to produce furfural rather than xylose, a) SNBMR treatment should be conducted at acid concentration (≥2wt%) and relatively low reaction temperatures (150-160°C); b) SBMR, kenaf, sunn hemp treatment require both higher acid concentrations (2wt%) and higher reaction temperatures (160°C), with the reaction time being as long as it would not lead to the degradation of pentose sugar backbone in all cases. Selective xylan hydrolysis to xylose should not be considered at temperatures significantly exceeding 160°C, particularly, at high acid concentrations.

4 Conclusion

A simplified two-step kinetic model adequately describes the hemicellulose hydrolysis of four crops at higher reaction temperatures (150-160°C) and acid concentrations (1-2 wt%). Though temperature and acid concentration exhibit a qualitatively similar influence on the rates of xylose formation and hydrolysis, the quantitative effects are different, thus affecting the trends in obtaining maximum xylose and furfural yield under varied reaction conditions. The Arrhenius activation energy values consistently increase with the biomass crystallinity index or both reactions. Effective reaction rate orders on acids of both xylose and furfural formation vary significantly for different crops increasing when the acid concentration exceeds 1 wt%. However, this increase occurs selectively for high-crystallinity biomasses and only for xylose formation, thus creating crop-specific scenarios if the yield of xylose is to be optimized. For feedstocks featuring a small difference in activation energy between xylose formation and degradation, pretreatment at low reaction temperatures with longer reaction times is particularly beneficial, compared to other crops.

[References]

[1] Dale B. Biofuels: Thinking clearly about the issues. Journal of Agriculture and Food Chemistry, 2008; 56(11): 3885–3891.

[2] Kumar R, Wyman C E. Cellulase adsorption and relationship to features of corstover solids produced by leading pretreatments. Biotechnology Bioengineering, 2009; 103(2): 252–67.

[3] Rawat R, Kumbhar B K, Tewari L. Optimization of alkali pretreatment for bioconversion of poplar (Populus deltoides) biomass into fermentable sugars using response surface methodology. Industrial Crops and Products, 2013; 44: 220–226.

[4] Zheng Y, Pan Z, Zhang R. Overview of biomass pretreatment for cellulosic ethanol production. International Journal of Agriculture and Biological Engineering, 2009; 2(3): 51–68.

[5] Dien B S, Sarath G, Pedersen J F, Sattler S E, Chen H, Harris D L, Nichols N N, Cotta M A. Improved sugar conversion and ethanol yield for forage sorghum (Sorghum bicolor L. Moench) lines with reduced lignin contents. Bioenergy Resources, 2009; 2(3): 153–164.

[6] Lynd L R, Elander R T, Wyman C E. Likely features and costs of mature biomass ethanol technology. Applied Biochemical Biotechnology, 1996; 57–58: 741–76.

[7] Degenstein J C, Kamireddy S R, Tucker M P, Ji Y. Novel batch reactor for the dilute acid pretreatment of lignocellulosic feedstocks with improved heating and cooling kinetics. International Journal of Chemical Reaction Engineering, 2011; A95: 1–9.

[8] Springer E L. Hydrolysis of aspenwood xylan with aqueous solutions of hydrochloric acid. Tappi, 1966; 49(3): 102–106.

[9] Lloyd T A, Wyman C E. Application of a depolymerization model for predicting thermochemical hydrolysis of hemicellulose. Applied Biochemical Biotechnology.2003; 105: 53–67.

[10] Saeman J F. Kinetics of wood sacharification: Hydrolysis of cellulose and decomposition of sugars in dilute acid at high temperature. Industrial Engineering and Chemistry Research, 1945; 37 (1): 43–52.

[11] Nabarlatz D, Farriol X, Montane D. Kinetic modeling of the autohydrolysis of lignocellulosic biomass for the production of hemicellulose- derived oligosaccharides. Industrial Engineering and Chemistry Research, 2004; 43: 4124–4131.

[12] Morinelly J E, Jensen J R, Browne M, Tomas B C, David R S. Kinetic characterization of xylose monomer and oligomer concentrations during dilute acid pretreatment of lignocellulosic biomass from forests residues and switchgrass. Industrial Engineering and Chemistry Research, 2009; 48(22): 9877–9884.

[13] Leu S Y, Zhu J Y. Substrate-related factors affecting enzymatic saccharification of lignocelluloses: our recent understanding. Bioenergy Research, 2012; 6: 405–415.

[14] Kamireddy S R, Li J, Abbina S, Berti M, Tucker M, Ji Y. Converting forage sorghum and sunn hemp into biofuels through dilute acid pretreatment. Industrial Crops and Products. 2013; 49: 598–609.

[15] Kamireddy S R, Kozliak E I, Tucker M, Ji Y. Determining the kinetics of sunflower hulls using dilute acid pretreatment in the production of xylose and furfural. Green Processing and Synthesis 2014; 3(1): 69–75.

[16] Lloyd T A, Wyman C E. Predicted effects of mineral neutralization and bisulfate formation on hydrogen ion concentration for dilute sulfuric acid pretreatment. Applied Biochemical Biotechnology, 2004; 115: 1013–1022.

[17] Scarlata C, Hyman D. Development and validation of a fast high pressure liquid chromatography method for the analysis of lignocelluloses biomass hydrolysis and fermentation products. Journal of Chromatography, 2010; 121: 2082–2087.

[18] Jensen J, Morinelly J, Aglan A, Mix A, Shonnard DR. Kinetic characterization of biomass dilute sulfuric acid hydrolysis: Mixtures of hardwoods, softwood, and switchgrass. Jounral of Americal Institute of Chemical Engineering, 2008; 54(6): 1637–1645.

[19] Kamireddy, S R, Degenstein J, Berti M, Ji Y. Pretreatment and Enzymatic Hydrolysis of Kenaf Biomass as a Potential Source for Lignocellulosic Biofuel and Green Chemicals. Journal of Current Organic Chemistry, 2013; 17(15): 1–9.

[20] Kamireddy, S R, Li J, Degenstein J, Tucker M, Ji Y. Effects and mechanism of metal chlorides salts on pretreatment and enzymatic digestibility of corn stover. Industrial Engineering and Chemistry Research, 2013; 52(5): 1775–1782.

[21] Aguilar R, Ramírez J A, Garrote G, Vázquez M. Kinetic study of acid hydrolysis of sugarcane bagasse. Journal of Food Engineering, 2002; 55: 309–318.

[22] Rodríguez-Chong A, Ramírez J A, Garrote G, Vázquez M. Hydrolysis of sugarcane bagasse using nitric acid: a kinetic assessment. Journal of Food Engineering, 2004; 61: 143–152.

[23] Demirbas A. Heavy metal adsorption onto agro-based waste materials: a review. Journal of Hazard Materials, 2008; 157: 220–229.

[24] Anthony J. Design of experiments of engineers and scientists, 1st edition. Buttworth- Heinemann, 2003; 36–37.

[25] Shen J, Wyman C E. A novel mechanism and kinetic model to explain enhanced xylose yields from dilute sulfuric acid compared to hydrothermal pretreatment of corn stover. Bioresource Technology, 2011; 102(19): 9111–9120.

[26] Zhou H, Zhu J Y, Luo X, Leu S Y, Wu X, Gleisner R, Dien B S, Hector R E, Yang D, Qiu X, Horn E, Negron J. Bioconversion of beetle-killed lodgepole pine using SPORL: process scale-up design, lignin coproduct, and high solids fermentationwithout detoxification. Industrial Engineering and Chemistry Research, 2013; 52(45): 16057–16065.

[27] Jin X J, Kamdem D P. Chemical composition, crystallinity and crystallite cellulose size in populus hybrids and aspen. Cellulose Chemistry and Technology, 2009; 43(7-8): 229–234.

[28] Sannigrahi P, Ragauskas A J, Tuskan G A. Poplar as a feedstock for biofuels: A review of compositional

characteristics. Biofuels Bioproducts Biorefinery, 2010; 4, 209–226.

[29] Wu Q, Meng Y, Concha K, Wang S, Li Y, Ma L, Fu S. Influence of temperature and humidity on nano-mechanical properties of cellulose nanocrystal films made from switchgrass and cotton. Industrial Crops and Products, 2013; 48: 28–35.

[30] Klinke H B, Thomsen A B, Ahring B K. Inhibition of ethanol-producing yeast and bacteria by degradation products produced during pre-treatment of biomass. Applied Microbiology. Biotechnology, 2004; 66: 10–26.

[31] Kalia S, Kumar A, Kaith BS, Sunn hemp cellulose graft copolymers polyhydroxybutyrate composites: morphological and mechanical studies. Advanced Material Letters, 2011; 2(1): 17–25.

[32] Theerarattananoon K, Wu X, Staggenborg S, Propheter J, Madl R, Wang D. Evaluation and characterization of sorghum biomass as feedstock for sugar production. American Society of Agricultural Biological Engineering, 2010; 53: 509–525.

[33] Jonoobi M, Harun J, Shakeri A, Misra M, Oksman K. Chemical composition, crystallinity and thermal degradation of bleached and unbleached kenaf bast (*Hibiscus cannabinus*) pulp and nanofibers. Bio Resources, 2009; 4(2): 626–639.

[34] Jacobsen SE, Wyman CE. Cellulose and hemicellulose hydrolysis models for application to current and novel pretreatment processes. Applied Biochemical and Biotechnology, 2000; 84–86: 81–96.